doi:10.1016/j.jmb.2010.12.019 J. Mol. Biol. (2011) 406, 215–227

Contents lists available at www.sciencedirect.com

Journal of Molecular Biology

journal homepage: http://ees.elsevier.com.jmb

# Construction of a Genetic Multiplexer to Toggle between Chemosensory Pathways in *Escherichia coli*

**Tae Seok Moon[1], Elizabeth J. Clarke[2], Eli S. Groban[2], Alvin Tamsir[3], Ryan M. Clark[4], Matthew Eames[2], Tanja Kortemme[2,5] and Christopher A. Voigt[1,2,3]***

[1]*Department of Pharmaceutical Chemistry, University of California, San Francisco, San Francisco, CA 94158, USA*
[2]*Graduate Group in Biophysics, University of California, San Francisco, San Francisco, CA 94158, USA*
[3]*Tetrad Program, University of California, San Francisco, San Francisco, CA 94158, USA*
[4]*City Arts and Technology High School, 301 De Montfort Avenue, San Francisco, CA 94112, USA*
[5]*Department of Biopharmaceutical Sciences, University of California, San Francisco, San Francisco, CA 94158, USA*

*Received 23 October 2010; received in revised form 5 December 2010; accepted 8 December 2010*
Available online 23 December 2010

***Edited by M. Gottesman***

***Keywords:***
genetic memory;
recombinase;
stochastic switching;
synthetic biology;
systems biology

Many applications require cells to switch between discrete phenotypic states. Here, we harness the FimBE inversion switch to flip a promoter, allowing expression to be toggled between two genes oriented in opposite directions. The response characteristics of the switch are characterized using two-color cytometry. This switch is used to toggle between orthogonal chemosensory pathways by controlling the expression of CheW and CheW*, which interact with the Tar (aspartate) and Tsr* (serine) chemoreceptors, respectively. CheW* and Tsr* each contain a mutation at their protein–protein interface such that they interact with each other. The complete genetic program containing an arabinose-inducible FimE controlling CheW/CheW* (and constitutively expressed *tar*/*tsr**) is transformed into an *Escherichia coli* strain lacking all native chemoreceptors. This program enables bacteria to swim toward serine or aspartate in the absence or in the presence of arabinose, respectively. Thus, the program functions as a multiplexer with arabinose as the selector. This demonstrates the ability of synthetic genetic circuits to connect to a natural signaling network to switch between phenotypes.

© 2010 Elsevier Ltd. All rights reserved.

## Introduction

Bacteria have mechanisms by which they can vary their DNA so that individuals within a population are performing different tasks. This heterogeneity is often achieved by enzymes that excise, invert, or rearrange the DNA. In a classical system, the cyanobacterium *Anabaena* forms filaments and, under nitrogen starvation, roughly every 10th cell differentiates to form nitrogen-fixing heterocysts. This is done via the excision of an 11- bp piece of DNA that causes cells to turn on nitrogenase/hydrogenase, turn off photosystem II, and undergo membrane and metabolic changes.[1] Similarly, the physical inversion of promoter directionality underlies the phase and antigenic variation that enables pathogens to evade the immune system.[2] Some organisms, such as the gut bacterium *Bacteroides*, have up to 30 such DNA invertases that form complex "shufflons".[3] In engineering cells, it would be useful to be able to program this heterogeneity such that cells within a population are performing different functions (e.g., different chemical transformations in a bioreactor).

*Corresponding author. Room 408C, 1700 4th Street, San Francisco, CA 94158, USA. E-mail address: cavoigt@picasso.ucsf.edu.

Abbreviations used: GFP, green fluorescent protein; RFP, red fluorescent protein; RBS, ribosome binding site; NSF, National Science Foundation.

0022-2836/$ - see front matter © 2010 Elsevier Ltd. All rights reserved.

Invertases, which change the orientation of DNA, have been incorporated into a number of synthetic genetic circuits. The cre/lox system has been used as a mechanism for site-directed gene insertion and deletion since the 1980's.[4] When the *lox*P sites are oriented in the same direction, Cre can also function

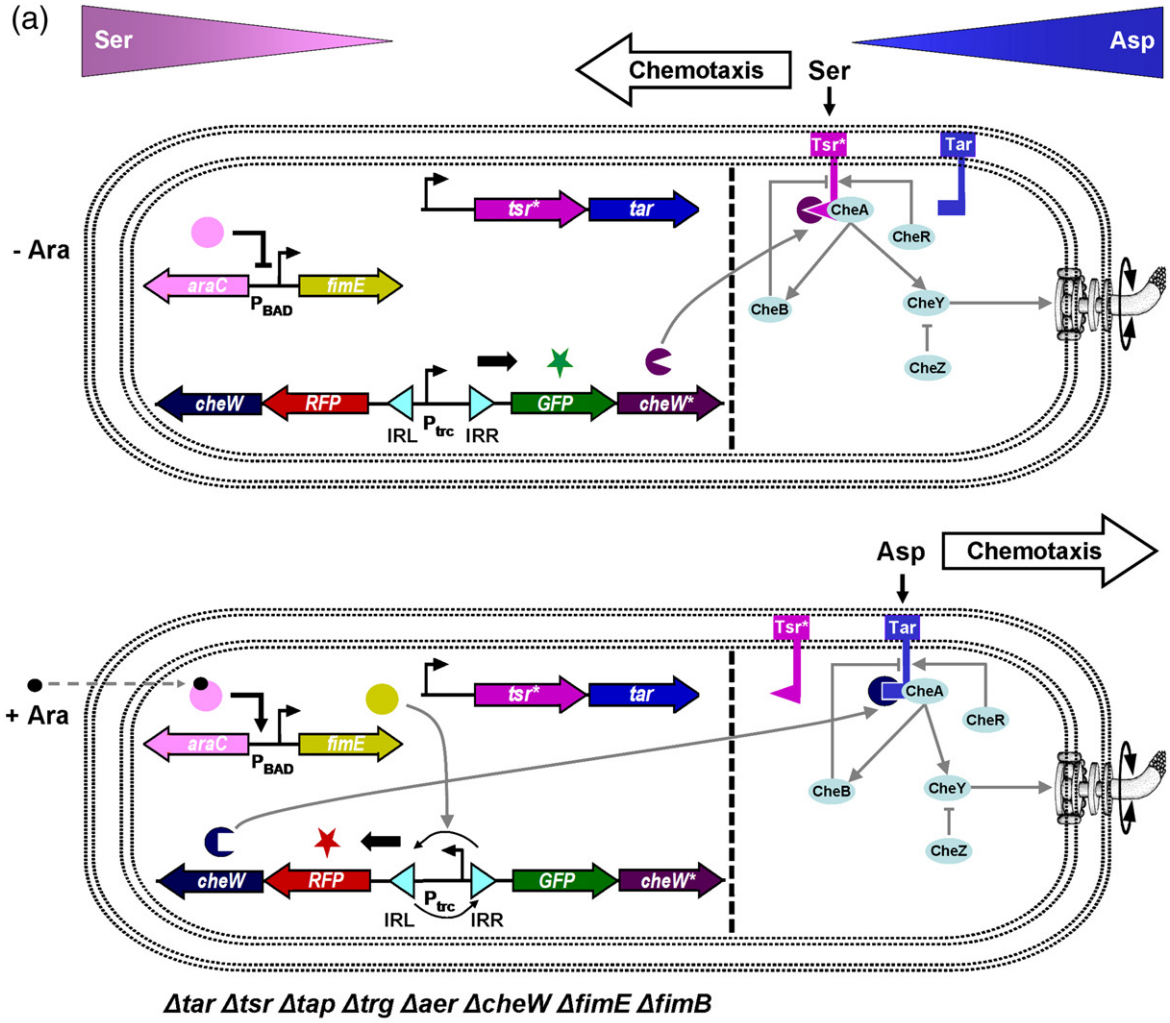


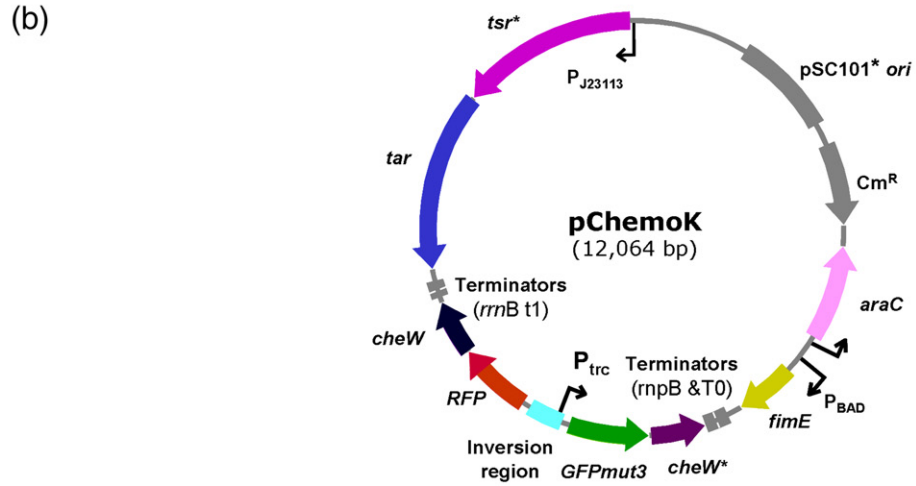


**Fig. 1** (*legend on next page*)

as an invertase. This system forms the core of a synthetic genetic counter, where a cascade of invertases are arranged to record a series of inducer pulses.[5] The Hin recombinase was used to construct a genetic program that solves the Hamiltonian path problem.[6] These recombinases are reversible, and this behavior can lead to instability in the switch. There are also invertases that are irreversible, where different proteins control the inversion in each direction. One of the most studied examples is the FimB–FimE pair that controls the phase variation of type 1 fimbriae in *Escherichia coli*.[7] The FimE protein causes the switch to occur in one direction with high fidelity, and FimB switches equally well between both states.[8,9] The FimE protein has been harnessed as part of a synthetic inducible system, where the inversion of promoters produces a switch with no basal activity.[10] The memory function can be enhanced by interdigitating the binding sites of multiple orthogonal invertases.[11] There are other regulatory interactions, including positive feedback loops and cross repression, which could switch between multiple states, but these mechanisms are less sharp, with a higher basal activity in the off state.[12,13]

It would be a useful tool for biotechnology to harness invertases to switch between multiple cellular phenotypes. By changing the orientation of a promoter, the invertase could switch between two phenotypes defined by two genes encoded in opposite orientations. However, it remains challenging to connect synthetic genetic circuits to the control of a cellular phenotype. One difficulty is the identification of simple control points that will produce a distinct phenotype and knowing (and being able to control) the dynamic range required to switch between states. Successful examples include the connection of a toggle switch to the control of biofilm formation,[14] a logic gate to the invasion of mammalian cells,[15,16] and quorum sensing to regulated cell death.[17] Sensors for cell–cell communication signals and small molecules (theophylline and an herbicide) have been connected to the control of flagellar rotation and swimming.[18–20]

In natural regulatory networks, there are a variety of mechanisms by which signals can be switched between pathways associated with different responses. This switching can occur via a scaffolding protein that aligns signaling proteins into a particular spatial arrangement.[21,22] This scaffolding allows signaling proteins to be shared between pathways while maintaining orthogonality. In eukaryotes, these scaffolds link membrane-bound receptors and ion channels to signal cascades. The pathways themselves often involve shared components. For example, two scaffolding proteins (c-Jun N-terminal kinase-interacting protein-1 and mitogen-activated protein kinase kinase kinase1) link different upstream signals to the activation of stress responses associated with the c-Jun N-terminal kinases.[23–25] This circuit has the potential to perform a function that is analogous to an electronic multiplexer, where multiple inputs can be channeled to a single output based on the state of a third input, referred to as a selector. For example, the selector could be a signal that determines which scaffold protein is expressed. Synthetic scaffolds have been built by recombining protein–protein interaction domains (e.g., Src homology 3 and PDZ domains) to create scaffolds that "rewire" the signaling proteins to build a new pathway.[26]

The regulatory network controlling *E. coli* chemotaxis is one of the well-studied models of signal transduction (Fig. 1a). Extracellular signals are sensed by a set of five receptors: Tar (aspartate), Tsr (serine), Trg (galactose/ribose), Tap (dipeptides), and Aer (oxygen).[27] These receptors assemble into large clusters that are predominantly located at the poles of the bacterium.[28,29] The CheW protein binds to all five receptors and acts as a scaffold protein to recruit CheA, whose phosphorylation is stimulated by the receptor. The phosphate is transferred to the cytoplasmic protein CheY, which controls flagellar rotation. In this way, CheW integrates the signal from multiple receptors into a single response.[30] Previously, a pair of mutations in CheW* (V108M) and Tsr* (E402A) was shown to produce an orthogonal pair, where the mutated proteins interact with each other but not with wild-type Tsr or CheW.[31] Note that, in this reference, the interactions are functional (i.e., recover activity), but the protein–protein interactions were not measured. In this work, we use this interaction to toggle between activating the serine-responsive Tsr* and aspartate-responsive Tar. An arabinose-inducible system serves as the selector by controlling an invertase that switches between the expression of CheW or CheW*.

In this paper, we present a genetic program that controls the activation of two chemosensory path-

**Fig. 1.** The synthetic switch and sensors can be interfaced with the natural signaling pathways to control bacterial chemotaxis. (a) Without arabinose (top), the engineered strain produces CheW* (along with GFPmut3), making the strain respond to and attracted toward serine (serine chemotaxis). With arabinose addition (bottom), FimE inverts the invertible region, triggering expression of CheW (along with RFP). CheW preferably interacts with Tar, and the strain switches to aspartate chemotaxis. While $P_{BAD}$ is an inducible promoter, $P_{trc}$ and $P_{J23113}$ used in this paper are constitutive promoters. The dotted line is drawn to show the synthetic parts and devices (left) and the natural signaling pathways (right). CheB (methylesterase), CheR (methyltransferase), and CheZ (phosphatase) are peripheral components of the natural chemotaxis system and they affect the concentration of phospho-CheY.[27] (b) A map of the pChemoK plasmid is shown.

ways by using an invertase-based switch to control the expression of orthogonal CheW adaptors (Fig. 1). First, we characterize the kinetics of the arabinose-inducible FimE switch on a low-copy plasmid such that it can be reliably connected to control cellular phenotypes. Then, the complete program is constructed, and chemotaxis experiments are performed in an *E. coli* strain, where all of the native chemoreceptors (methyl-accepting chemotaxis proteins) are knocked out of the genome. Codon-optimized Tar and Tsr* are expressed from a constitutive promoter, allowing both to be independently optimized and continuously present on the cell membrane. Their activation depends on the expression of either the CheW or the CheW* adaptor protein, which changes the attractant to which the bacteria swim.

## Results

### Characterization of the *fim* switch using two-color flow cytometry

Previously, Ham *et al.* constructed a synthetic switch based on the FimE invertase.[10] The circuit was carried on a high-copy plasmid (pFIP, pBR322 ori), and FimE was expressed by the arabinose-inducible $P_{BAD}$ promoter. A constitutively active version of the $P_{trc}$ promoter was placed between the FimE binding sites (IRL and IRR). Its orientation is flipped upon the addition of arabinose, and this leads to the expression of green fluorescent protein (GFP). Using a fluorimeter, the authors have shown that the switch starts to turn on after 3 h and is fully induced by 6 h. The circuit was also shown to operate as memory, where a pulse of inducer irreversibly turns on the switch, as measured up to 8 h. Surprisingly, the circuit was shown to function in a strain of *E. coli* where *fimBE* was still present in the genome. LB medium was used for these experiments.

The invertase switch should be able to toggle between two genes oriented in opposite directions. To test this, we constructed a plasmid based on pFIP, where GFPmut3 is expressed in the initial orientation, and red fluorescent protein (RFP) after the promoter is inverted (Fig. 2a). The plasmid backbone was changed to a lower-copy pSC101* origin as toxicity and cloning instability was observed at a higher copy. In addition, the *fimBE* genes were knocked out of *E. coli* (Materials and Methods). As shown in a previous work,[10] we were able to turn the switch on stably in cells containing the *fimBE* genes during exponential phase in LB medium. However, we observed reverse switching when the cells were grown in poor medium and in exponential phase. Notably, when the cells were plated post-switching, nearly equal numbers of colonies appeared red and green, and some colonies had spots of both colors (not shown). All of these issues were resolved once the native *fimBE* genes were knocked out of the chromosome.

Experiments were performed, where the gain of RFP and the loss of GFP were measured after the addition of arabinose to LB medium. The steady-state transfer function of the switch is shown as a function of arabinose concentration (after 6 h) (Fig. 2b). Full switching occurred at relatively low concentrations of inducer (0.04 mM). However, the decline in GFP signal occurred slowly as a function of inducer concentration. Interestingly, at intermediate concentrations, the two-color cytometry distribution showed that there are two distinct populations of cells (Fig. 2d, center top panel). Both show maximum green fluorescence, but some cells are completely on with respect to red fluorescence, whereas others are completely off. This indicates that, in some cells, there is a mixed population of switched and unswitched plasmids. In contrast, at maximum arabinose induction (5 mM), all of the cells contain fully switched plasmids (Fig. 2d, right top panel).

The temporal behavior of the switch was also measured (Fig. 2c). At maximum induction, the switch begins to turn on after 2 h and then is fully induced by 6 h, thus agreeing with the previous measurements.[10] The two-color cytometry distributions also show a graded transition from the green to the red states, where the intermediate time point (4 h) represents intermediate levels of both fluorescent proteins (Fig. 2d). This shows that all of the plasmids contain inverted promoters, and this time point represents the delay in expression of RFP and degradation of GFP.

The chemotaxis assay requires minimal media because a complex medium, such as LB, could interfere with the serine or aspartate gradient. Many applications would require that the switch operate in microenvironments under similar, less optimal growth conditions. To measure the effect of different media, we measured the switch dynamics in minAaa medium, which is used for the chemotaxis experiments (Materials and Methods). The doubling time of the *E. coli* strain is 130 min in minAaa (5 mM arabinose), as opposed to 50 min in LB (5 mM arabinose). An eightfold-higher inducer concentration (0.3 mM) is required to obtain complete switching at steady state (Fig. 2e). In addition, the switch is much slower, requiring 16 h for complete conversion (Fig. 2f). Complete switch inversion was also confirmed by DNA sequencing of plasmids obtained from randomly sampled cells following a 16-h induction in minAaa medium. There are several mechanisms that could cause the switch to be slower, including lower expression of FimE or changes in the plasmid copy number.

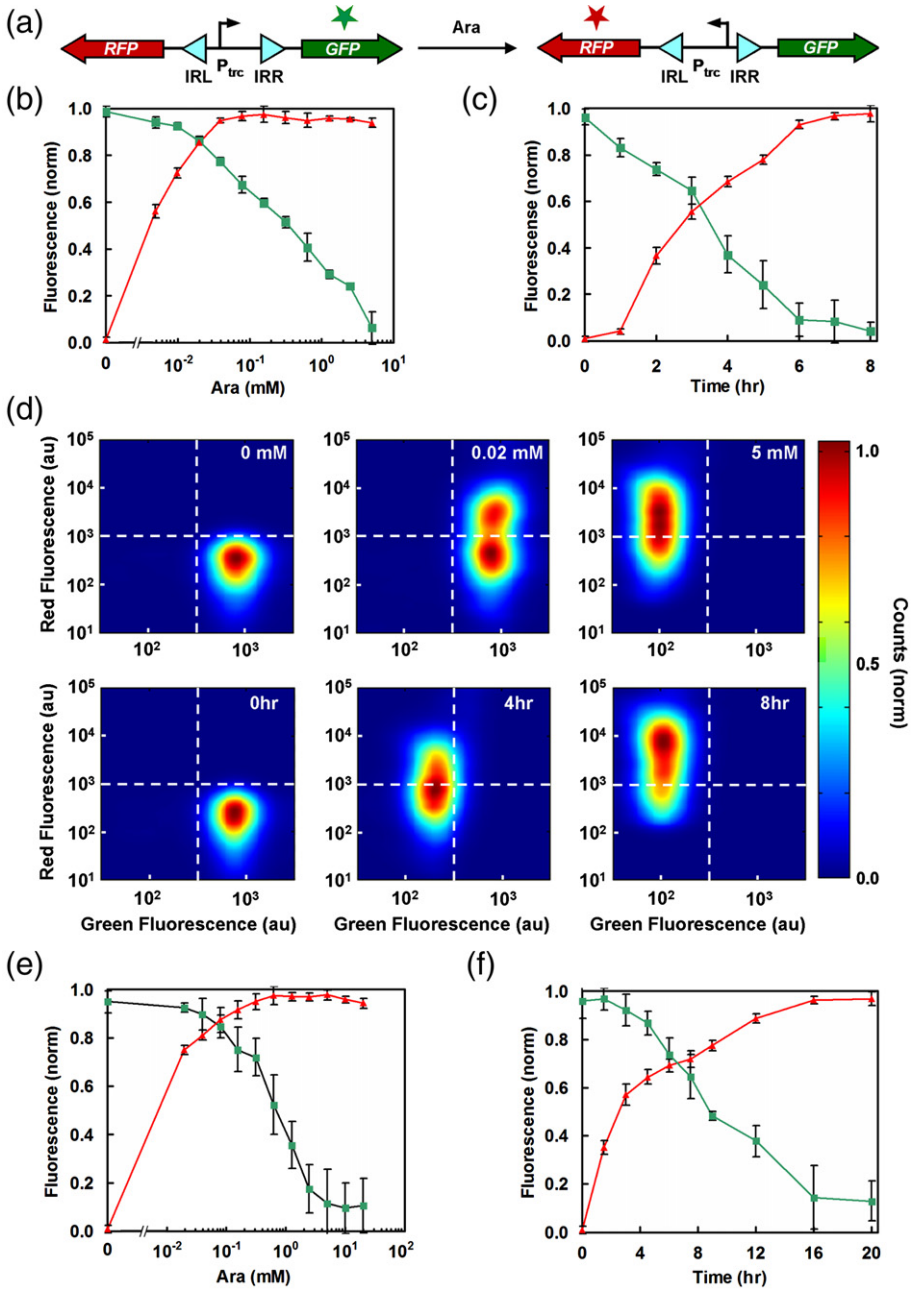


**Fig. 2.** Characterization of the *fim* switch using two-color flow cytometry. (a) GFPmut3 (green) and RFP (red) were placed on either side of the *fim* invertible region. (b–f) FimE-promoted switching occurred more quickly in LB medium than in minAaa medium. (▲) The average RFP fluorescence (normalized); (■) the average GFPmut3 fluorescence (normalized). Normalization was done by the following formula: $[\log(F)-\log(F_B)]/[\log(F_M)-\log(F_B)]$, where $F$, $F_B$, and $F_M$ are sample, background, and maximum fluorescence levels, respectively. The background fluorescence values were obtained from control cells lacking the fluorescent protein genes (CAV8). Data are the averages and standard deviations of three replicates. (b) Cultures in LB medium with 6 h of induction. (c) Cultures in LB medium containing 5 mM arabinose (see Fig. S2 for the $OD_{600}$ data). (d) Two-color flow cytometry data are shown for cultures in LB medium. (Top) Cultures were induced for 6 h with 0 mM arabinose (left), 0.02 mM arabinose (middle), and 5 mM arabinose (right). (Bottom) Cultures were induced with 5 mM arabinose for 0 h (left), 4 h (middle), and 8 h (right). The dotted lines are drawn as a guide to the eye, separating the green (lower right), red (upper left), and green/red (upper right) regions. (e) Cultures in minAaa medium with 16 h of induction. (f) Cultures in minAaa medium containing 5 mM arabinose (see Fig. S2 for the $OD_{600}$ data).

## Genetic program design and optimization

In *E. coli*, the five chemotaxis receptors (Tar, Tsr, Tap, Trg, and Aer) form two-dimensional clusters in the membrane that are preferentially targeted to the poles (or "nose") of the bacterium.[32,33] The formation of clusters amplifies the signal, produces increased sensitivity and cooperativity in the response, and is involved in signal adaptation.[34,35] As such, the signaling dynamics are sensitive to the ratios of the receptor concentrations (e.g., Tsr signaling depends on the abundance of Tar and Tap).[36,37] The clusters are also very stable, and the exchange of Tar receptors is much slower than cell division, whereas CheW and CheA are exchanged on the order of 5–10 min.[38] Based on this, our design approach for synthetic chemosensors is to constitutively express the receptors, such that they are intended to form a uniform cluster integrated in the membrane. This allows the expression levels of the receptors and the signaling to be optimized once for the cluster. Which receptors are active is determined by which orthogonal CheW adaptor is expressed. Our system only has two receptors (Tar and Tsr*), but this approach could also scale for the construction of more complex multi-receptor synthetic clusters that incorporate homologous or chimeric receptors[39–42] or those that have been engineered or evolved to respond to new molecules.[43]

The adaptor protein CheW interacts with all five receptors to recruit CheA. Previously, a CheW variant (CheW*) with a single mutation (V108M) that disrupts its interaction with wild-type Tsr was identified.[31] The interaction was recovered by making a single compensating mutation in Tsr (E402A) to create Tsr*. The CheW*–Tsr* pair recovers 70% of wild-type activity on a swarm plate. The non-cognate CheW–Tsr* interaction only recovers 25%, implying that Tsr* preferentially interacts with CheW*. Homologous recombination is a potential concern when combining CheW and CheW* onto a single plasmid. To avoid this problem, we used whole-gene DNA synthesis to build a codon-optimized *cheW** that shares only 78% nucleotide identity with the native *cheW* sequence (79% with the codon-optimized *cheW* sequence), and the mutations are distributed throughout the sequence (Supplementary Information).[44]

One of the challenges in optimizing this genetic program was obtaining functional expression levels for Tar:CheW and Tsr*:CheW*. High concentrations of CheW or chemoreceptors have been shown to inhibit chemotactic ability.[31,37,45] The first constructs produced expression levels that were too high, which led to toxicity and instability when cloned into the pFIP plasmid backbone. Moving to a low-copy pSC101* plasmid reduced these problems. The original design also oriented the *tsr**–*tar* operon in the same direction as *cheW*, and it was transcribed by a strong constitutive promoter ($P_{lacIQ}$). To reduce *tar* and *tsr** expression, we placed a very weak constitutive promoter ($P_{J23113}$, BBa_J23113)† upstream of a strong ribosome binding site (RBS) (rbs0 from the Weiss set).[46] Further, toxicity was observed after arabinose induced the FimE-driven promoter flip, which was determined to be due to read-through from the terminators after *cheW* (rrnB: t1). This was eliminated by orienting the *tsr**–*tar* operon in the opposite direction to *cheW*. The concentration of CheW also impacts the regulatory network, both through the ratio with CheA and its role in organizing the receptor clusters.[47,48] For CheW and CheW*, a weak RBS (rbs2 from the Weiss set) was paired with the constitutive promoter $P_{trc}$, which gets inverted by the *fim* switch. The final construct is shown in Fig. 1b, and sequence details are presented in Materials and Methods and in Supplementary Information.

Wild-type *E. coli* possesses genes encoding all five native chemoreceptors and a gene encoding CheW. All six genes (*tar*, *tsr*, *tap*, *trg*, *aer*, and *cheW*) were knocked out of the *E. coli* BW28357 chromosome (Materials and Methods) to eliminate interference from native chemotaxis pathways. In addition, the wild-type genes encoding the *fim* recombinase proteins (*fimE* and *fimB*) were knocked out to eliminate possible aberrant switching (previous section). Rich medium cannot be used for amino acid chemotaxis assays because it complicates the creation of an amino acid gradient. However, the strain containing all the knockouts and the pChemoK plasmid did not grow well in minimal A medium. Methionine, histidine, leucine, and threonine do not interfere with chemotaxis, and supplementation with these amino acids restored growth (minAaa medium).

## Chemotaxis experiments

The multiplexer toggles between the activation of Tsr* and Tar with the addition of arabinose, causing the bacteria to change from moving toward serine to aspartate. Chemotaxis is measured using a plate-based assay developed by Goulian *et al.* (Fig. 3, and a detailed assay is presented in Supplementary Information).[43,49] The only significant change is that more agar is added to the medium, which, in our hands, produces less dramatic results but reduces day-to-day variability. Briefly, a gradient of aspartate or serine is created by spotting 10 μl of 10 mM attractant on semisolid agar at 7-mm intervals down the center of a square plate (81 $cm^2$). The gradient is stabilized by drying the plates at 4 °C for 16 h.

† http://partsregistry.org

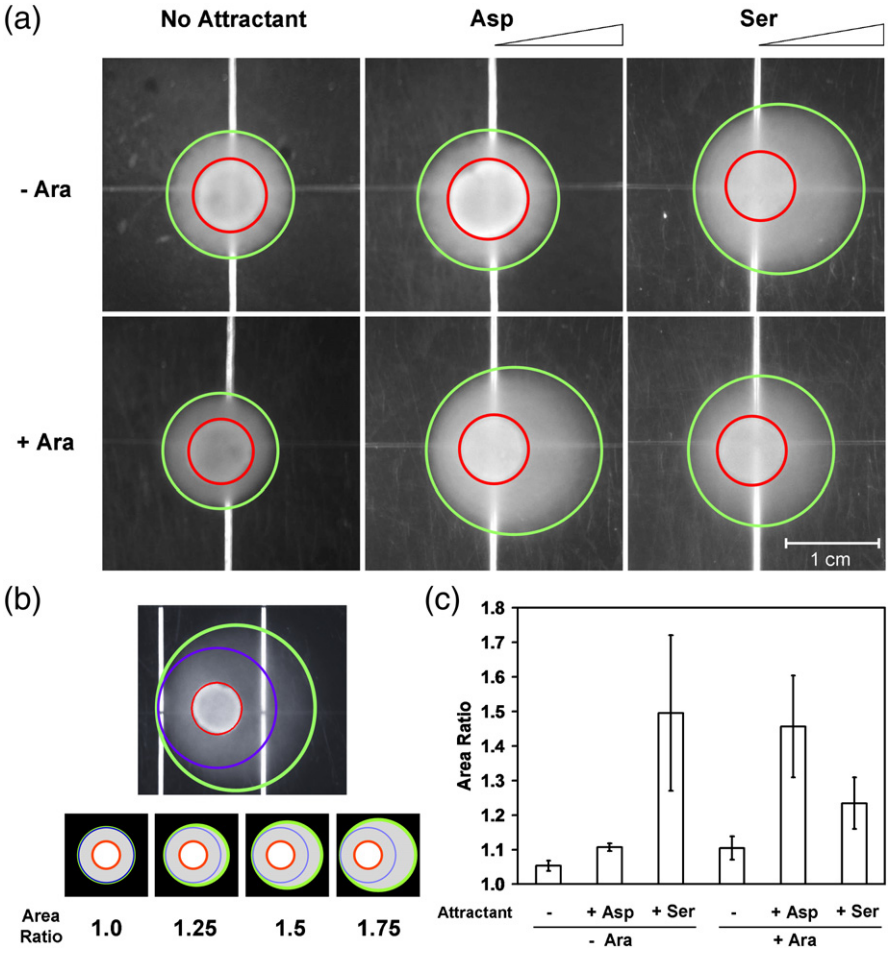


**Fig. 3.** Assays for bacterial chemotaxis. (a) A gradient of aspartate or serine was created by spotting 10 μl of 10 mM attractant on semisolid agar (on the right sides of these images). Cultures were induced with 5 mM arabinose (bottom) or supplemented with 0.5% (w/v) glucose in order to repress potential leaky expression of $P_{BAD}$ (top). Those shown are representative images of experiments that were performed at least three times. Red circles and green ovals were computationally generated as described in Fig. 3b. (b) Image analysis was carried out using a MATLAB® algorithm. (Top) Red circles indicate the positions where 10 μl of the culture was placed, and green ovals indicate the entire regions formed by bacterial chemotaxis. The regions surrounded by blue circles are assumed to be formed by random walks only. (Bottom) The area ratio is defined as the green oval area divided by the blue circle area. Bacteria executing random walks only would result in an area ratio of 1, whereas chemotactic bacteria attracted toward aspartate or serine would lead to a higher area ratio. Schematic images are shown for four area ratio values to serve as a guide. (c) Quantitative analysis of bacterial chemotaxis. Data are the averages and standard deviations of three images taken from experiments performed on different days. No attractant spotted (−); 10 μl of 10 mM aspartate spotted (+Asp); and 10 μl of 10 mM serine spotted (+Ser). Uninduced (−Ara) and induced (+Ara).

The state of the *fim* switch is set prior to the chemotaxis assay. Cells are grown in minAaa medium in culture tubes for 16 h at 37 °C, either in the presence of 5 mM arabinose (+Ara) or of 0.5% (w/v) glucose to repress $P_{BAD}$ (−Ara). Then, cells are diluted into minAaa medium in the absence of glucose to promote the expression of flagella.[50,51] After 1 h of growth, 10 μl of the culture is spotted onto the plate. After 48 h at 30 °C, the plates are photographed, and the halos formed by the bacteria are quantified using custom image processing software (Materials and Methods). Like the classic swarm plate, a halo is formed by chemotactic bacteria. The halo is circular if the bacteria are swimming in random directions and appears as an oval oriented toward the gradient if the bacteria are swimming biased toward the attractant. This is quantified by the software as the ratio of the surface area of the observed oval to that of a perfect circle (Fig. 3b). Bacteria lacking chemotactic abilities would lead to an area ratio of 1, whereas bacteria showing directional bias would result in a higher area ratio. This procedure enables us to quantify the standard deviation between plates.

When the *fim* switch is not activated (−Ara), the bacteria swim toward serine (Fig. 3a and c). This is

due to the expression of CheW*, which preferentially binds to Tsr*. There is no response seen in the absence of attractant or in the presence of aspartate. When the *fim* switch is activated (+Ara), then CheW is expressed, which preferentially binds to Tar, and the bacteria move toward aspartate. There is some cross reactivity between CheW and Tsr*, which leads to small but reproducible chemotaxis to serine. This is consistent with previous results with this orthogonal pair, where the swarm rate of a CheW/Tsr* strain retained 25% of the wild-type rate.[31] Residual CheW* could also contribute to such chemotaxis to serine.

The behavior of the genetic program was further investigated by knocking out individual components and assaying the impact on chemotaxis. The quantitative data are shown in Fig. 4, and examples of the plates are shown in Supplementary Information. When *cheW* is deleted, Tar is inactive, and cells are not able to swim toward aspartate after the addition of arabinose (Fig. 4a). In the absence of arabinose, there is no effect on the response, as expected. The elimination of *tar* has a similar effect, where cells no longer move toward aspartate after the addition of arabinose (Fig. 4b).

When *cheW** is deleted, Tsr* is inactive, and the cells do not show chemotaxis to serine in the absence of arabinose (Fig. 4c). After the addition of arabinose, the response is identical with the complete program. When *tsr** is deleted, chemotaxis toward serine is eliminated, both with and without the addition of arabinose (Fig. 4d). There is no impact on

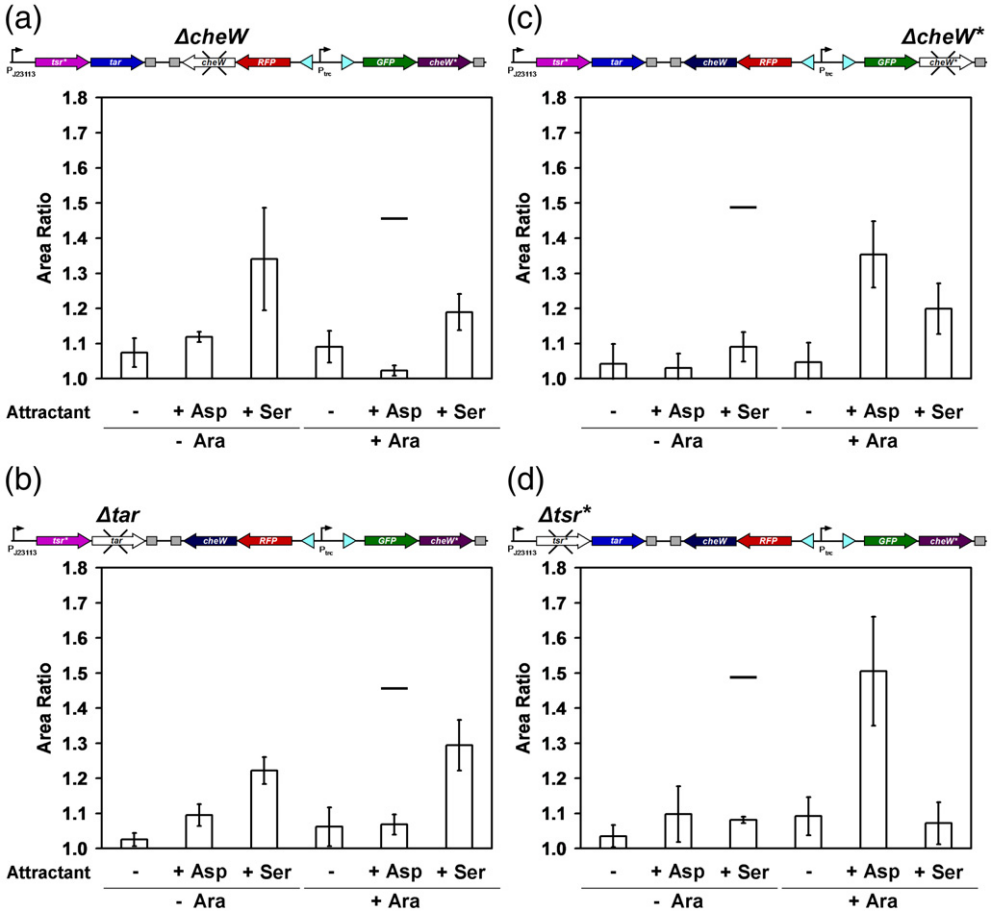


**Fig. 4.** Analysis of genetic program with various genes knocked out. The four deletion mutants lack one of the four genetic parts required for the orthogonal chemotaxis signaling, and chemotaxis assays using these mutants were carried out as described in Fig. 3. Data are the averages and standard deviations of three images taken from three experiments performed on three different days (for representative images, see Supplementary Information). The black lines, indicating the average values from Fig. 3c, are drawn to serve as a comparison guide. No attractant spotted (−Ara) and induced (+Ara). (a) Chemotaxis assays using the *cheW* deletion mutant. The remaining CheW* after *fim* switching may result in the higher area ratio than expected (+Ser +Ara). (b) Chemotaxis assays using the *tar* deletion mutant. Cross talk between Tsr* and CheW increases significantly when the cognate partner Tar does not exist (+Ser +Ara). (c) Chemotaxis assays using the *cheW** deletion mutant. Cross talk between Tsr* and CheW was confirmed in the absence of *cheW** (+Ser +Ara). (d) Chemotaxis assays using the *tsr** deletion mutant. No cross talk between Tar and CheW* (+Asp −Ara) was observed.

the remainder of the responses. There is no observed cross talk between Tar and CheW* even when Tsr*, the cognate chemoreceptor for CheW*, is removed.

The chemotaxis toward serine that is observed in the +Ara state in the complete program is Tsr* dependent. However, chemotaxis toward serine is reduced, but not eliminated, when CheW is deleted (Fig. 4a). This implies that residual CheW* remains active, following *fim* inversion. Indeed, even after 16 h of induction, the *fim* switch is sufficiently slow, where a significant fraction of the cells would have recently switched (Fig. 2f). Further, growth in this medium is slow, and this reduces the dilution rate. To examine this effect, we serially subcultured the cells without induction for additional 39 h prior to the plate assay. This eliminated the serine response after the 16-h induction with arabinose (area ratio = 1.10 ± 0.06).

## Discussion

Here, we have built a multiplexer using an invertase-based switch that can toggle between chemosensory signaling pathways in response to a chemical inducer. Multiplexers are used in electronic systems to share devices and to reduce resource requirements. This advantage is evident in the genetic program constructed here, where most of the chemotaxis signal proteins are shared between pathways, as opposed to having all of the proteins duplicated to create two orthogonal pathways. We demonstrated that synthetic CheW variants with orthogonal protein–protein interactions with Tar and mutated Tsr can be used to toggle between continuously expressed surface receptors. When these CheW variants are under differential regulatory control, these form a 2-to-1 multiplexer, where a selector (in our program, arabinose) toggles between two inputs. Multiplexers are often coupled with demultiplexers (single input switched between multiple outputs) in communications as a cost-saving measure to reduce the number of required channels.

*E. coli* has one of the simpler chemosensory systems, with five chemoreceptors and one CheW. A survey of the sequenced genomes of microorganisms showed that 65% of 206 organisms with related systems have multiple CheW homologues.[52] *Geobacter sulfurreducens* has one of the more complex systems with 34 Tar, 10 CheW, 4 CheA, and 25 CheY homologues.[53] The multiple CheW (and CheA) homologues in a single organism could behave as a multiplexer if they are under differential regulatory control. This appears to occur in *Rhodobacter*, where different CheW homologues mediate chemotaxis during aerobic photoheterotrophic growth.[54] In this way, shifts in environmental conditions could lead to switching between active receptors more quickly without having to completely reassemble the stable and highly organized receptor clusters. Following the circuit analogy, the control of the expression of CheW homologues acts as the multiplexer, and the control over CheY homologues could function as a demultiplexer.

The application of protein engineering to create orthogonal pairs is a generalizable approach to pathway engineering.[55] Classically, this is done by randomly mutagenizing one protein, screening for a loss of function, and then randomly mutagenizing the second protein, screening for a suppressor mutation. This approach led to the discovery of the Tsr*/CheW* mutations.[31] This pair of single mutations produces orthogonal pathways, but there remains a small, but significant, amount of cross talk between CheW and Tsr* (which was not explicitly selected against in the original mutagenesis experiments). New approaches in computational design and bioinformatics have yielded orthogonal pairs with reduced cross-reactions. Structure-guided computational methods have been able to predict mutations that alter interaction specificity by designing and repacking side chains at the protein–protein interface.[56,57] Skerker *et al.* have applied mutual information analysis to compare multiple sequence alignments to identify those amino acids at the protein–protein interface that determine specificity.[58] Using this approach, they were able to identify a triple mutant of EnvZ that switched its interaction partner from OmpR to RstB. In addition to the thermodynamics of the protein–protein binding interactions, natural pathways have kinetic mechanisms to reduce cross talk. A histidine kinase can act as a phosphatase, eliminating any inadvertent cross-phosphorylation.[59–61]

Invertases have a number of properties that are desirable for the construction of genetic circuits. They produce discrete switch events with zero basal state, which can be irreversible, and represent a mechanism for cellular memory that can be maintained even after cell death. As such, they have been incorporated in a counter[5] and here, a multiplexer. The interdigitation of the binding sites of multiple invertases could be a powerful mechanism to store information. However, there are some drawbacks to these systems. Bidirectional invertases (e.g., *cre* and *flp*) could produce instabilities, where continued expression causes the DNA to flip back and forth.[62] The unidirectional invertases (e.g., *fimE*) require a second protein to flip in the opposite direction, but these proteins (e.g., *fimB*) are not unidirectional.[8,9] This property impedes circuits that need to cycle switching between the two states. The circuits are also very slow to switch, requiring 6 h in LB and 16 h in minimal medium. This slow switching behavior limits their ability to be layered into more complex circuits. For example, the counter required 2 days to count to three.[5] Finally, we

observe stochastic switching at intermediate induction, where individual cells contain plasmids in different states. Directed evolution has already been used to create orthogonal invertases and mutants with improved thermostability and to improve the efficiency and unidirectionality of recombinases.[63–67]

Natural populations of bacteria use similar mechanisms to diversify their function in a microenvironment or as a bet-hedging strategy. There are a number of potential applications in biotechnology that could harness programmable prokaryotic differentiation. For example, in the division of labor during fermentation, different subpopulations of cells could be dedicated to different tasks such as the breakdown of biomass or the formation or sequestration of product.[68] Bacteria could be engineered to seek and destroy various toxic chemicals in response to local concentration gradient,[18] and stochastic switching might lead to spontaneous allocation of different pollution areas to different subpopulations of cells. Our work represents a step toward the construction of complex networks, which will be essential for greater control over a broader range of cellular processes and differentiation.

## Materials and Methods

### Strains and growth media

*E. coli* strain DH10B was used for all molecular biology manipulations. Cells were grown in either LB medium (Miller, BD Biosciences, San Jose, CA) or minimal A medium[49] supplemented with 0.2% (v/v) glycerol, 1 mM $MgSO_4$, 0.5 mM $CaCl_2$, 0.2 mM $ZnSO_4$, and 2 mg/ml each of methionine, histidine, leucine, and threonine (minAaa medium). Semisolid agar was made from the minAaa medium with 0.3% (w/v) agar (BD Biosciences, San Jose, CA). Kanamycin (20 μg/ml), ampicillin (100 μg/ml), and chloramphenicol (34 μg/ml) were added as appropriate.

*E. coli* strain BW28357 ($F^-$ Δ(*araD-araB*)*567* Δ*lacZ4787* (::rrnB-3) $\lambda^-$ Δ(*rhaD-rhaB*)*568 hsdR514*) was obtained from the Coli Genetic Stock Center at Yale, and the knockout strain (CAV8) with eight chromosomal genes deleted (*tar*, *tsr*, *tap*, *trg*, *aer*, *cheW*, *fimE*, and *fimB*) was constructed from BW28357 by λ *red*-mediated recombination and subsequent P1 transduction.[69] The position numbers of each gene in *E. coli* MG1655 are as follows: *trg* (1,490,494–1,492,134), *tap* (1,967,407–1,969,008), *tar* (1,969,054–1,970,715), *cheW* (1,970,860–1,971,363), *aer* (3,215,578–3,217,098), *fimB* (4,538,980–4,539,582), *fimE* (4,540,060–4,540,656), and *tsr* (4,589,680–4,591,335). The kanamycin resistance marker was removed using pCP20,[69] and each knockout was confirmed by DNA sequencing.

### Plasmid construction

The plasmid pChemoK ($Cm^r$ and pSC101* origin), containing the *fim* switch and the two orthogonal signaling systems for bacterial chemotaxis (Fig. 1), was constructed from synthetic DNA (DNA 2.0, Menlo Park, CA) and the one-step isothermal DNA assembly method.[70] Construction of the *fim* switch was based on the pFIP plasmid.[10] The two orthogonal signaling systems were constructed using optimized synthetic genes encoding Tar, Tsr*, CheW, and CheW* (for their DNA sequences, see Supplementary Information). The amino acid sequence for RFP was based on monomeric RFP,[71] and its codon-optimized gene was synthesized. The gene for GFPmut3 and pSC101* origin were from the *psicA_gfp* reporter[72] and BBa_I50042,[1] respectively. RBSs and promoters were tuned in order to balance expression levels of chemosensory pathway genes. For *cheW* and *cheW**, we paired a weak synthetic RBS (TCACACAGGAAAGGCCTCG, rbs2 from the Weiss set)[46] with the constitutive promoter $P_{trc}$.[10] For *tar* and *tsr** expression, we placed a very weak constitutive promoter $P_{J23113}$ (BBa_J23113, CTGATGGCTAGCTCAG-TCCTAGGGATTATGCTAGC)[1] upstream of a strong synthetic RBS (ATTAAAGAGGAGAAATTAAGC, rbs0 from the Weiss set).[46] The full pChemoK plasmid was assembled using the one-step isothermal DNA assembly method[70] and was used both for the two-color cytometry (Fig. 2) and chemotaxis experiments (Fig. 3). The four deletion mutants that lack one of the four genetic parts required for the orthogonal chemotaxis signaling (*tar*, *tsr**, *cheW*, and *cheW**) were constructed from pChemoK using the one-step isothermal DNA assembly method.[70]

### Flow cytometry

Cultures induced with arabinose (0–20 mM; 0–20 h) were diluted using phosphate buffered saline (pH 7) supplemented with 2 mg/ml kanamycin, and flow cytometry data were obtained using a BD Biosciences LSRII flow cytometer (BD Biosciences, San Jose, CA). The data were gated by forward and side scatter, and each data set consisted of at least 10,000 cells. FlowJo (TreeStar Inc., Ashland, OR) was used for data analysis and compensation. For compensation, singly stained samples were collected from green cells (i.e., cells uninduced, top left of Fig. 2d) or red cells (i.e., cells fully induced, bottom right of Fig. 2d). To measure autofluorescence background, we used the strain CAV8. Normalization used for Fig. 2 was performed by the following formula: $[\log(F) - \log(F_B)]/[\log(F_M) - \log(F_B)]$, where $F$, $F_B$, and $F_M$ are sample, background, and maximum fluorescence levels, respectively. Figure 2d was plotted using "smoothhist2D" function of MATLAB® (The MathWorks, Inc., Natick, MA) with the following parameters: 30 for λ smoothing factor, 500 × 500 for bin size, and 0.001 for outlier cutoff.

### Chemotaxis assays and image analysis

Plate-based chemotaxis assays were performed as described by Goulian *et al.*[43,49] A detailed protocol is included in Supplementary Information. Briefly, a gradient of aspartate or serine was created by spotting 10 μl of 10 mM attractant (either aspartate or serine) on semisolid agar with ~ 7-mm spacings down the middle of the square plate (81 $cm^2$), and the plates were then dried at 4 °C for 16 h. Cultures were either induced with 5 mM arabinose or supplemented with 0.5% (w/v) glucose, which served to repress potential sporadic expression of

$P_{BAD}$. After a 16-h culture at 37 °C and 250 rpm (in the presence or in the absence of arabinose), we washed and diluted cells into an $OD_{600}$ of 0.2 using minAaa medium supplemented with 34 μg/ml chloramphenicol. These diluted cultures were grown (in the absence of glucose and arabinose) for an additional 1 h and then were spotted 13.5, 20, and 27 mm from the center line of attractant. Images were taken using AlphaImager® equipped with Computar TV Zoom Lens (Cell Biosciences, Santa Clara, CA) after 48 h of incubation at 30 °C. The distance between lens and plate was 50 cm, and exposure time was 0.06–0.12 s Plate position and zoom lens were adjusted to cover 27 mm × 27 mm with the spot position to the center of each image.

Image analysis was performed using a MATLAB® algorithm that calculates the area of the entire swarm region resulting from bacterial chemotaxis (green ovals in Fig. 3b) and compares it to that of a circle corresponding to an equivalent unbiased random walks (blue circles in Fig. 3b). The blue circle is centered on the red circle corresponding to the location of the initial spotting (Fig. 3b), and the blue circle's radius reflects the distance from its center to the nearest point on the corresponding green oval. The area ratio was defined as the area of the green oval divided by that of the blue circle. Bacteria lacking chemotactic abilities would lead to an area ratio of 1, whereas bacteria showing directional bias would result in a higher area ratio. To identify the inner red circle, we converted the image into a black-and-white image ("im2bw") using a threshold value of 0.7. Holes in the processed image were filled using "imfill" function. The perimeters of the inner colony trace were smoothed out using "imerode" followed by "imdilate" functions. The coordinates of the perimeter boundary were extracted from this processed image using "bwtraceboundary" function. This coordinates were then fitted using least-square method to obtain the fitted circle/ellipse equation. The same procedure was repeated (changing the threshold value down to 0.25 in the first step) to identify the "halo" region. All the image analysis functions are from Image Processing toolbox of MATLAB®.

Supplementary materials related to this article can be found online at doi:10.1016/j.jmb.2010.12.019

## Acknowledgements

We thank Ala Trusina and Patrick Visperas for the initial work as part of the 2006 University of California, San Francisco iGEM team. We thank Adam Arkin (University of California, Berkeley), John Parkinson (The University of Utah), and Mark Goulian (University of Pennsylvania) for the materials and help with assays. DNA 2.0 graciously provided synthesis for the University of California, San Francisco iGEM project. C.A.V. was supported by the Pew and Packard Foundations, Office of Naval Research, National Institutes of Health (EY016546 and AI067699), National Science Foundation (NSF) (BES-0547637), and a Sandler Family Opportunity Award. C.A.V. and T.K. are part of the NSF Synthetic Biology Engineering Research Center. T.K. was supported by the Sloan Foundation, an NSF CAREER award, and a Sandler Family Award.

## References

1. Golden, J. W., Robinson, S. J. & Haselkorn, R. (1985). Rearrangement of nitrogen fixation genes during heterocyst differentiation in the cyanobacterium *Anabaena*. *Nature*, **314**, 419–423.
2. van der Woude, M. W. & Baumler, A. J. (2004). Phase and antigenic variation in bacteria. *Clin. Microbiol. Rev.* **17**, 581–611.
3. Cerdeno-Tarraga, A. M., Patrick, S., Crossman, L. C., Blakely, G., Abratt, V., Lennard, N. *et al.* (2005). Extensive DNA inversions in the *B. fragilis* genome control variable gene expression. *Science*, **307**, 1463–1465.
4. Sternberg, N. & Hamilton, D. (1981). Bacteriophage P1 site-specific recombination. I. Recombination between *lox*P sites. *J. Mol. Biol.* **150**, 467–486.
5. Friedland, A. E., Lu, T. K., Wang, X., Shi, D., Church, G. & Collins, J. J. (2009). Synthetic gene networks that count. *Science*, **324**, 1199–1202.
6. Baumgardner, J., Acker, K., Adefuye, O., Crowley, S. T., Deloache, W., Dickson, J. O. *et al.* (2009). Solving a Hamiltonian Path Problem with a bacterial computer. *J. Biol. Eng.* **3**, 11.
7. Klemm, P. (1986). Two regulatory fim genes, fimB and fimE, control the phase variation of type 1 fimbriae in *Escherichia coli*. *EMBO J.* **5**, 1389–1393.
8. Gally, D. L., Bogan, J. A., Eisenstein, B. I. & Blomfield, I. C. (1993). Environmental regulation of the fim switch controlling type 1 fimbrial phase variation in *Escherichia coli* K-12: effects of temperature and media. *J. Bacteriol.* **175**, 6186–6193.
9. McClain, M. S., Blomfield, I. C. & Eisenstein, B. I. (1991). Roles of fimB and fimE in site-specific DNA inversion associated with phase variation of type 1 fimbriae in *Escherichia coli*. *J. Bacteriol.* **173**, 5308–5314.
10. Ham, T. S., Lee, S. K., Keasling, J. D. & Arkin, A. P. (2006). A tightly regulated inducible expression system utilizing the *fim* inversion recombination switch. *Biotechnol. Bioeng.* **94**, 1–4.
11. Ham, T. S., Lee, S. K., Keasling, J. D. & Arkin, A. P. (2008). Design and construction of a double inversion recombination switch for heritable sequential genetic memory. *PLoS One*, **3**, e2815.
12. Becskei, A., Seraphin, B. & Serrano, L. (2001). Positive feedback in eukaryotic gene networks: cell differentiation by graded to binary response conversion. *EMBO J.* **20**, 2528–2535.
13. Gardner, T. S., Cantor, C. R. & Collins, J. J. (2000). Construction of a genetic toggle switch in *Escherichia coli*. *Nature*, **403**, 339–342.
14. Kobayashi, H., Kaern, M., Araki, M., Chung, K., Gardner, T. S., Cantor, C. R. & Collins, J. J. (2004). Programmable cells: interfacing natural and engineered gene networks. *Proc. Natl Acad. Sci. USA*, **101**, 8414–8419.
15. Anderson, J. C., Clarke, E. J., Arkin, A. P. & Voigt, C. A. (2006). Environmentally controlled invasion of

cancer cells by engineered bacteria. *J. Mol. Biol.* **355**, 619–627.
16. Anderson, J. C., Voigt, C. A. & Arkin, A. P. (2007). Environmental signal integration by a modular AND gate. *Mol. Syst. Biol.* **3**, 133.
17. You, L., Cox, R. S., III, Weiss, R. & Arnold, F. H. (2004). Programmed population control by cell–cell communication and regulated killing. *Nature*, **428**, 868–871.
18. Sinha, J., Reyes, S. J. & Gallivan, J. P. (2010). Reprogramming bacteria to seek and destroy an herbicide. *Nat. Chem. Biol.* **6**, 464–470.
19. Topp, S. & Gallivan, J. P. (2007). Guiding bacteria with small molecules and RNA. *J. Am. Chem. Soc.* **129**, 6807–6811.
20. Weiss, L. E., Badalamenti, J. P., Weaver, L. J., Tascone, A. R., Weiss, P. S., Richard, T. L. & Cirino, P. C. (2008). Engineering motility as a phenotypic response to LuxI/R-dependent quorum sensing in *Escherichia coli*. *Biotechnol. Bioeng.* **100**, 1251–1255.
21. Pawson, T. & Scott, J. D. (1997). Signaling through scaffold, anchoring, and adaptor proteins. *Science*, **278**, 2075–2080.
22. Zeke, A., Lukács, M., Lim, W. A. & Reményi, A. (2009). Scaffolds: interaction platforms for cellular signalling circuits. *Trends Cell Biol.* **19**, 364–374.
23. Dickens, M., Rogers, J. S., Cavanagh, J., Raitano, A., Xia, Z., Halpern, J. R. *et al.* (1997). A cytoplasmic inhibitor of the JNK signal transduction pathway. *Science*, **277**, 693–696.
24. Garrington, T. P. & Johnson, G. L. (1999). Organization and regulation of mitogen-activated protein kinase signaling pathways. *Curr. Opin. Cell Biol.* **11**, 211–218.
25. Xu, S. & Cobb, M. H. (1997). MEKK1 binds directly to the c-Jun N-terminal kinases/stress-activated protein kinases. *J. Biol. Chem.* **272**, 32056–32060.
26. Park, S. H., Zarrinpar, A. & Lim, W. A. (2003). Rewiring MAP kinase pathways using alternative scaffold assembly mechanisms. *Science*, **299**, 1061–1064.
27. Baker, M. D., Wolanin, P. M. & Stock, J. B. (2006). Signal transduction in bacterial chemotaxis. *BioEssays*, **28**, 9–22.
28. Gestwicki, J. E. & Kiessling, L. L. (2002). Inter-receptor communication through arrays of bacterial chemoreceptors. *Nature*, **415**, 81–84.
29. Gosink, K. K., Buron-Barral, M. C. & Parkinson, J. S. (2006). Signaling interactions between the aerotaxis transducer Aer and heterologous chemoreceptors in *Escherichia coli*. *J. Bacteriol.* **188**, 3487–3493.
30. Bourret, R. B. & Stock, A. M. (2002). Molecular information processing: lessons from bacterial chemotaxis. *J. Biol. Chem.* **277**, 9625–9628.
31. Liu, J. D. & Parkinson, J. S. (1991). Genetic evidence for interaction between the CheW and Tsr proteins during chemoreceptor signaling by *Escherichia coli*. *J. Bacteriol.* **173**, 4941–4951.
32. Maddock, J. R. & Shapiro, L. (1993). Polar location of the chemoreceptor complex in the *Escherichia coli* cell. *Science*, **259**, 1717–1723.
33. Greenfield, D., McEvoy, A. L., Shroff, H., Crooks, G. E., Wingreen, N. S., Betzig, E. & Liphardt, J. (2009). Self-organization of the *Escherichia coli* chemotaxis network imaged with super-resolution light microscopy. *PLoS Biol.* **7**, e1000137.
34. Keymer, J. E., Endres, R. G., Skoge, M., Meir, Y. & Wingreen, N. S. (2006). Chemosensing in *Escherichia coli*: two regimes of two-state receptors. *Proc. Natl Acad. Sci. USA*, **103**, 1786–1791.
35. Endres, R. G. & Wingreen, N. S. (2006). Precise adaptation in bacterial chemotaxis through "assistance neighborhoods". *Proc. Natl Acad. Sci. USA*, **103**, 13040–13044.
36. Sourjik, V. & Berg, H. C. (2004). Functional interactions between receptors in bacterial chemotaxis. *Nature*, **428**, 437–441.
37. Liu, J. D. & Parkinson, J. S. (1989). Role of CheW protein in coupling membrane receptors to the intracellular signaling system of bacterial chemotaxis. *Proc. Natl Acad. Sci. USA*, **86**, 8703–8707.
38. Schulmeister, S., Ruttorf, M., Thiem, S., Kentner, D., Lebiedz, D. & Sourjik, V. (2008). Protein exchange dynamics at chemoreceptor clusters in *Escherichia coli*. *Proc. Natl Acad. Sci. USA*, **105**, 6403–6408.
39. Kwon, O., Georgellis, D. & Lin, E. C. (2003). Rotational on-off switching of a hybrid membrane sensor kinase Tar-ArcB in *Escherichia coli*. *J. Biol. Chem.* **278**, 13192–13195.
40. Michalodimitrakis, K. M., Sourjik, V. & Serrano, L. (2005). Plasticity in amino acid sensing of the chimeric receptor Taz. *Mol. Microbiol.* **58**, 257–266.
41. Utsumi, R., Brissette, R. E., Rampersaud, A., Forst, S. A., Oosawa, K. & Inouye, M. (1989). Activation of bacterial porin gene expression by a chimeric signal transducer in response to aspartate. *Science*, **245**, 1246–1249.
42. Ward, S. M., Delgado, A., Gunsalus, R. P. & Manson, M. D. (2002). A NarX–Tar chimera mediates repellent chemotaxis to nitrate and nitrite. *Mol. Microbiol.* **44**, 709–719.
43. Derr, P., Boder, E. & Goulian, M. (2006). Changing the specificity of a bacterial chemoreceptor. *J. Mol. Biol.* **355**, 923–932.
44. Villalobos, A., Ness, J. E., Gustafsson, C., Minshull, J. & Govindarajan, S. (2006). Gene Designer: a synthetic biology tool for constructing artificial DNA segments. *BMC Bioinformatics*, **7**, 285.
45. Cardozo, M. J., Massazza, D. A., Parkinson, J. S. & Studdert, C. A. (2010). Disruption of chemoreceptor signaling arrays by high level of chew, the receptor-kinase coupling protein. *Mol. Microbiol.* **75**, 1171–1181.
46. Weiss, R. (2001). *Cellular Computation and Communications Using Engineered Genetic Regulatory Networks.* Massachusetts Institute of Technology, Cambridge, MA.
47. Boukhvalova, M. S., Dahlquist, F. W. & Stewart, R. C. (2002). CheW binding interactions with CheA and Tar. Importance for chemotaxis signaling in *Escherichia coli*. *J. Biol. Chem.* **277**, 22251–22259.
48. Levit, M. N., Grebe, T. W. & Stock, J. B. (2002). Organization of the receptor–kinase signaling array that regulates *Escherichia coli* chemotaxis. *J. Biol. Chem.* **277**, 36748–36754.
49. Goldberg, S. D., Derr, P., DeGrado, W. F. & Goulian, M. (2009). Engineered single- and multi-cell chemotaxis pathways in *E. coli*. *Mol. Syst. Biol.* **5**, 283.
50. Adler, J. & Templeton, B. (1967). The effect of environmental conditions on the motility of *Escherichia coli*. *J. Gen. Microbiol.* **46**, 175–184.

51. Lai, H. C., Shu, J. C., Ang, S., Lai, M. J., Fruta, B., Lin, S. *et al.* (1997). Effect of glucose concentration on swimming motility in enterobacteria. *Biochem. Biophys. Res. Commun.* **231**, 692–695.
52. Hamer, R., Chen, P. Y., Armitage, J. P., Reinert, G. & Deane, C. M. (2010). Deciphering chemotaxis pathways using cross species comparisons. *BMC Syst. Biol.* **4**, 3.
53. Tran, H. T., Krushkal, J., Antommattei, F. M., Lovley, D. R. & Weis, R. M. (2008). Comparative genomics of *Geobacter* chemotaxis genes reveals diverse signaling function. *BMC Genomics*, **9**, 471.
54. Martin, A. C., Wadhams, G. H. & Armitage, J. P. (2001). The roles of the multiple CheW and CheA homologues in chemotaxis and in chemoreceptor localization in *Rhodobacter sphaeroides*. *Mol. Microbiol.* **40**, 1261–1272.
55. Mandell, D. J. & Kortemme, T. (2009). Computer-aided design of functional protein interactions. *Nat. Chem. Biol.* **5**, 797–807.
56. Kortemme, T., Joachimiak, L. A., Bullock, A. N., Schuler, A. D., Stoddard, B. L. & Baker, D. (2004). Computational redesign of protein–protein interaction specificity. *Nat. Struct. Mol. Biol.* **11**, 371–379.
57. Bolon, D. N., Grant, R. A., Baker, T. A. & Sauer, R. T. (2005). Specificity *versus* stability in computational protein design. *Proc. Natl Acad. Sci. USA*, **102**, 12724–12729.
58. Skerker, J. M., Perchuk, B. S., Siryaporn, A., Lubin, E. A., Ashenberg, O., Goulian, M. & Laub, M. T. (2008). Rewiring the specificity of two-component signal transduction systems. *Cell*, **133**, 1043–1054.
59. Alves, R. & Savageau, M. A. (2003). Comparative analysis of prototype two-component systems with either bifunctional or monofunctional sensors: differences in molecular structure and physiological function. *Mol. Microbiol.* **48**, 25–51.
60. Groban, E. S., Clarke, E. J., Salis, H. M., Miller, S. M. & Voigt, C. A. (2009). Kinetic buffering of cross talk between bacterial two-component sensors. *J. Mol. Biol.* **390**, 380–393.
61. Siryaporn, A. & Goulian, M. (2008). Cross-talk suppression between the CpxA–CpxR and EnvZ–OmpR two-component systems in *E. coli*. *Mol. Microbiol.* **70**, 494–506.
62. Voigt, K., Izsvak, Z. & Ivics, Z. (2008). Targeted gene insertion for molecular medicine. *J. Mol. Med.* **86**, 1205–1219.
63. Buchholz, F., Angrand, P. O. & Stewart, A. F. (1998). Improved properties of FLP recombinase evolved by cycling mutagenesis. *Nat. Biotechnol.* **16**, 657–662.
64. Buchholz, F. & Stewart, A. F. (2001). Alteration of Cre recombinase site specificity by substrate-linked protein evolution. *Nat. Biotechnol.* **19**, 1047–1052.
65. Santoro, S. W. & Schultz, P. G. (2002). Directed evolution of the site specificity of Cre recombinase. *Proc. Natl Acad. Sci. USA*, **99**, 4185–4190.
66. Sarkar, I., Hauber, I., Hauber, J. & Buchholz, F. (2007). HIV-1 proviral DNA excision using an evolved recombinase. *Science*, **316**, 1912–1915.
67. Oberdoerffer, P., Otipoby, K. L., Maruyama, M. & Rajewsky, K. (2003). Unidirectional Cre-mediated genetic inversion in mice using the mutant *loxP* pair *lox66/lox71*. *Nucleic Acids Res.* **31**, e140.
68. Steen, E. J., Kang, Y., Bokinsky, G., Hu, Z., Schirmer, A., McClure, A. *et al.* (2010). Microbial production of fatty-acid-derived fuels and chemicals from plant biomass. *Nature*, **463**, 559–562.
69. Datsenko, K. A. & Wanner, B. L. (2000). One-step inactivation of chromosomal genes in *Escherichia coli* K-12 using PCR products. *Proc. Natl Acad. Sci. USA*, **97**, 6640–6645.
70. Gibson, D. G., Young, L., Chuang, R. Y., Venter, J. C., Hutchison, C. A., III & Smith, H. O. (2009). Enzymatic assembly of DNA molecules up to several hundred kilobases. *Nat. Methods*, **6**, 343–345.
71. Campbell, R. E., Tour, O., Palmer, A. E., Steinbach, P. A., Baird, G. S., Zacharias, D. A. & Tsien, R. Y. (2002). A monomeric red fluorescent protein. *Proc. Natl Acad. Sci. USA*, **99**, 7877–7882.
72. Temme, K., Salis, H., Tullman-Ercek, D., Levskaya, A., Hong, S. H. & Voigt, C. A. (2008). Induction and relaxation dynamics of the regulatory network controlling the type III secretion system encoded within *Salmonella* pathogenicity island 1. *J. Mol. Biol.* **377**, 47–61.